DC RAILWAY LINE VOLTAGE RIPPLE FOR PERIODIC AND APERIODIC PHENOMENA

Andrea Mariscotti

DINAEL – Dept. of Naval and Electrical Eng., Univ. of Genova, Via Opera Pia 11A - 16145 Genova – Italy, andrea.mariscotti@unige.it

Abstract: The dc voltage fluctuation (sometimes referred to as ripple) is considered for the pantograph voltage on dc railways. Some indexes and processing techniques are considered to evaluate steady state and transient phenomena: Ripple Index based on time and frequency domain expressions, DFT and wavelet analysis.

Key words: Power Quality, Time domain analysis, Spectral analysis, Guideway Transportation Systems, Conducted Interference

1. INTRODUCTION

A general problem for railways is that of electrical interoperability, that aims at ensuring the safe and efficient circulation of trains across different railway networks in different countries, such as those of European Union. Even if the preferred lines for high speed interconnection over Europe are the ac railway lines either 25 kV 50 Hz or 15 kV 16.7 Hz), dc railway lines are part of the problem in several ways: they can be used for interconnection of high speed lines to bring the vehicles into stations in those countries with a traditional dc railway network; they are however considered as conventional lines and interoperability applies also to them with slightly reduced requirements; the free circulation of rolling stock from different operators even at a local geographical scale demands however to consider some of the electrical interoperability issues. Besides power quality issues related to harmonic disturbance, network resonance and network-rolling stock interaction [1], a very basic requirement that impacts on train performance and service efficiency is the voltage level "seen" by the train pantograph, called useful voltage. The useful voltage $U_{av,u}$ is defined in the EN 50388 [2] for dc railway systems as the average value of the mean value of pantograph voltage V_p (i.e. dc component) over a well defined geographical area of the national network and for one or several trains. Thus, there is distinction between the $U_{av,u}$(zone), for the average operated over all the circulating trains in a given zone, and $U_{av,u}$(train), for the average operated for one train over a predetermined journey or its timetable. The measurement data used for the following analysis were recorded on the Italian dc 3 kV network (the conventional line, not the high speed line) within the activities of the EU project RAILCOM during 2008 [1].

2. USEFUL VOLTAGE AND RIPPLE INDEX

$U_{av,u}$ is the power supply index that is evaluated to assess the adequacy of the infrastructure (power supply network) to the prescribed performance of the circulating rolling stock. For dc 3 kV railways the minimum $U_{av,u}$ is set to 2800 V for high speed lines and 2700 V for conventional lines.

In this work the attention is not on the simple calculation of the useful voltage, but on the identification of steady and transient fluctuations. Transients are relevant for many reasons and often they need to be detected and isolated over long recordings. The reasons for transients may be:

- (Type 1) unusual sudden tractive efforts with packet-like current absorptions may trigger oscillations in the onboard filter current and thus in the pantograph current I_p, but with negligible effect on V_p, due to the low short circuit impedance of the network;
- (Type 2) change over to an adjacent supply section connected to a different substation, passing under a neutral section and producing a V_p step change;
- (Type 3) pantograph bounces disconnect the sliding contact from the contact wire for a few ms, depending on several factors (speed, mechanical performance of the pantograph frame and dampers, catenary oscillations); this produces a step change of absorbed current I_p and a spike like change of V_p;
- (Type 4) change of operating conditions and spectrum of current emissions of onboard converters due to various reasons: wheel slip, internal control rules, driving style and applied torque, etc.

Ripple is defined as the variation of a quantity about its steady state value during steady electric system operation [3]. Ripple is interpreted often as a periodic variation around the steady state dc value, but not necessarily so [4][5]: some components are related to steady periodic sources (harmonics of rectifiers and inverters [6]-[8] in steady conditions), but others are caused by transients (interpreted as aperiodic phenomena or abrupt changes of the said converters operating conditions).

The complex scenario of variable operating conditions and position of the rolling stock and the possibility of local unstable conditions of sets of traction converters located on different nearby vehicles, give rise to a wide class of

transients related to the inrush current of the vehicle filter, pantograph bounces, wheel slipping and sliding, etc.

The mathematical approach described in [9] is summarized here just for reader's convenience. Given the $q(t)$ quantity (in this case the pantograph voltage), the peak-to-peak value q_{pp} over k_T samples interval is the exact ripple index and is given by:

$$q_{pp,T} = \max_{n,k}\{q[n] - q[n+k+k_T]\} \quad (1)$$

The exact quantification of the ripple index (RI) is extremely time consuming, so a spectrum based approach was followed. The spectrum $Q[k]$ is computed on a time window of duration T (set to 0.1 s in [9]) and a sliding DFT approach is followed for transients, similarly to [10][11], to evaluate the power quality indexes for aperiodic signals.

RI is then calculated as the sum of the components of index k with amplitude larger than a given threshold *thr*, defined by the set K_{thr}; Sum-of-Amplitudes (SA) and Sum-of-Amplitudes-and-Phases (SAP) rules were shown in [9]:

$$q_{DFT,T,SA} = \sum_{k\in K_{thr}} |Q[k]| \qquad q_{DFT,T,SAP} = \left| \sum_{k\in K_{thr}} Q[k] \right| \quad (2)$$

The *thr* value must be carefully chosen not to leave out any significant component and to keep the size of K_{thr} as low as possible. The largest peak for each components group (of amplitude $2\delta f$) was isolated by a *PeakDetect*() function and used for the computation of (2). A threshold $thr=10^{-5}$ was able to include all the relevant components of the test signals in [9]. With respect to the amplitude of the used test signals the relative threshold value is then about 10^{-3}, in agreement with the spectral components normal retained for harmonic analysis. The optimal overlap factor p was shown to be either 0.25 or 0.5 and the latter is generally preferable for best performance in terms of correlation between adjacent spectra, in particular for the Hanning window.

3. REAL CASES

Recordings taken on the Italian 3 kV dc railway lines are considered to evaluate the RI, to identify the transients, their spectral characteristics and their influence on the $U_{av,u}$.

Transients and their frequency spectra are relevant not only for the contribution to the overall PQ problem, but also for interference to track circuits [12][15]. Here only the first issue is considered, but the same technique may be applied to I_p to isolate transients during signalling interoperability tests.

3.1. Reference values

A 10 min profile of pantograph voltage and current is shown in Fig. 1, together with a first calculation of SA and SAP indexes, that on this temporal scale result mostly overlapped. This recording shows quite a regular profile of current absorption and the large step changes in V_p are due to neutral sections (Type 1 transient). The V_p box like increase after point (2) is probably due to a particular arrangement approaching a station, confirmed by the sudden decrease of I_p at the end of the shown recording.

A fairly constant I_p profile at large values represents medium/high speed traveling on straight lines with rare stops, such as on main lines.

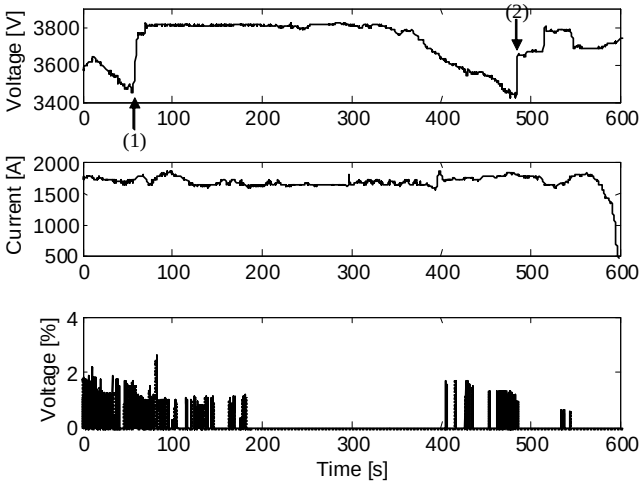

Figure 1. Results of a preliminary evaluation of SA (black solid) and SAP (black dotted) for a 10 min test run

The Fig. 1 above shows the pantograph voltage profile of a heavy loaded line, where the absorbed current is in the range of 1700-1800 A, corresponding to an absorbed power of about 5.8 to 6.3 MW. The corresponding voltage ripple is however limited to 2%, occurring in some time intervals.

3.2. Frequency domain analysis

In Fig. 2 (obtained as a zoom of an apparently almost steady state operating interval) a step change in voltage RI can be observed at time t^*=5.8 s, with time resolution limited by the selected time window T for DFT analysis. The change is due to an increase of some of the spectral components (Type 4). Transients of this kind produce several non-characteristic components that are often the reason for non compliance with signalling interference limits [12] and must be correctly weighted in the overall operating profile of the converter under test [13].

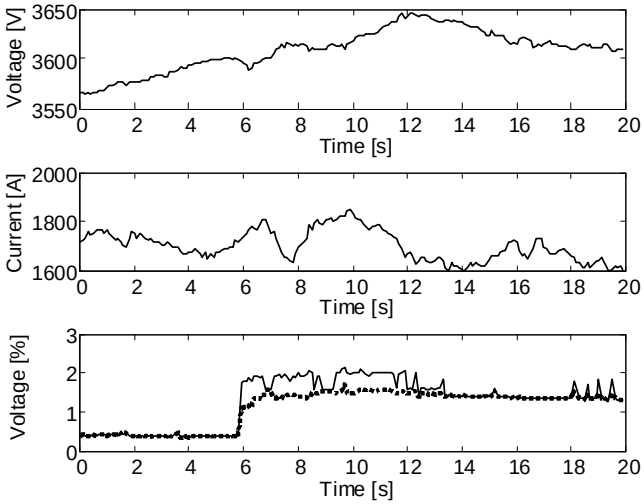

Figure 2. RI step change at t^*=5.8 s; SA (solid) and SAP (dotted)

The RI step change may be produced by both low frequency leakage components (Type 1 transient) and higher frequency characteristic and non-characteristic harmonics (Type 4 transient), as shown in Fig. 3: in Fig. 3(a) two components at 150 and 480 Hz definitely increase after t^*, besides an evident frequency leakage below 80 Hz; in Fig. 3(b) the dotted and solid black spectra at or after t^* prevail, showing an increase also of high frequency components. Two components are almost fix, 300 Hz (due to the substation) and 550 Hz (due to the onboard chopper, i.e. front-end dc/dc converter) with respect to the time axis and to the adopted frequency resolution. On the contrary, for a finer resolution of 5 Hz, the low frequency profile shows an irregular profile that does not correspond to a real harmonic pattern, but rather to fluctuations also in relationship to the free response of the on-board filter.

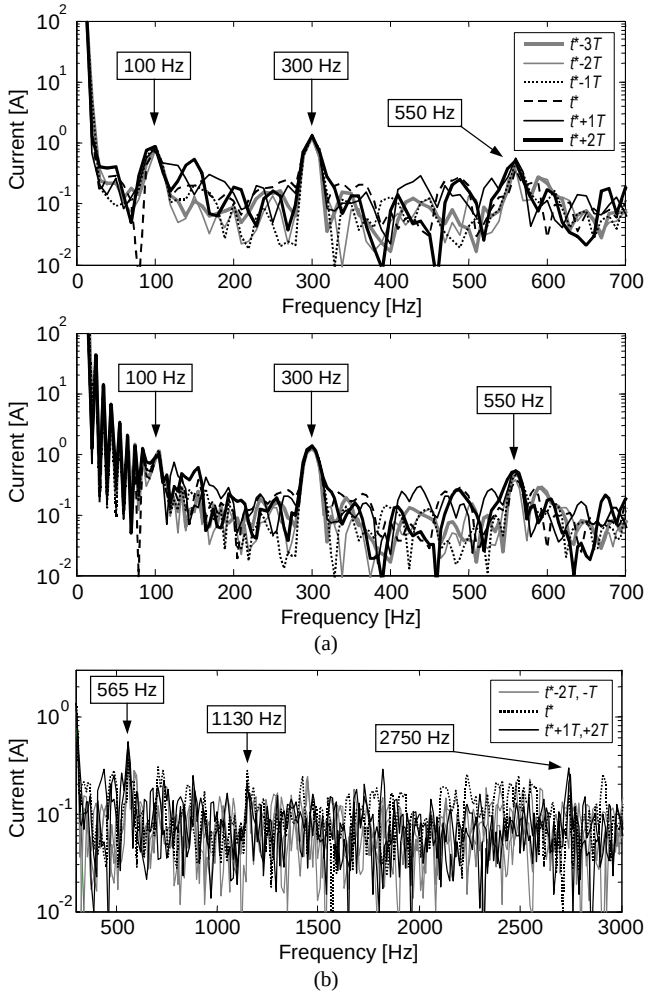

Figure 3. Analysis of transient behavior at t^*=5.8 s (a) low frequency, with base and enhanced frequency resolution; (b) high frequency

In many cases the raw Fourier spectra need to be pre-processed before being used for the RI evaluation and other large scale computations. Since the background noise is very large and may contribute largely to the calculation of an overall index like RI or the total rms, it is often advisable to set a threshold to zero out the components below it. When evaluating broad peaks at fine resolution, peak isolation is necessary to avoid counting them more than once, including lateral components due to leakage. These techniques were already successfully adopted while processing records of electromagnetic field intensity on-board rolling stock [14].

As it is well known, transients leave a clear signature in the Fourier spectra computed by Short Time Fourier Transform, or *spectrogram*, approach. An example is shown in Fig. 4, where the steady characteristic harmonics at 300, 600 and 900 Hz may be easily seen, as well as some others in the higher frequency interval. In Fig. 4(b) time-varying components may be seen at about 80 s between 1700 and 2200 Hz reducing to 1250 to 1550 Hz at 170 s, indicating a long brake; the estimated rate is about 5-5.5 Hz/s.

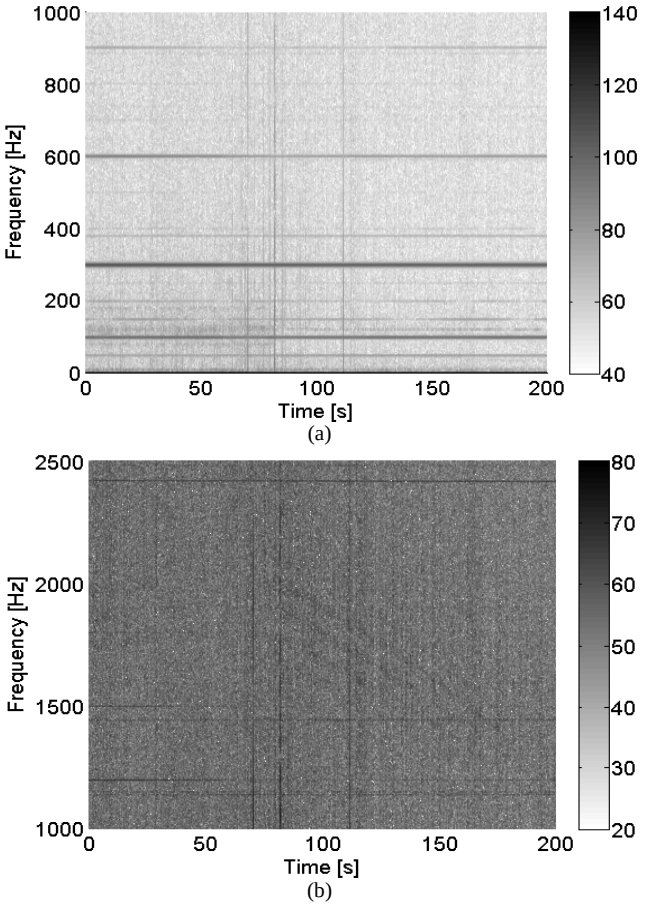

Figure 4. Spectrogram: (a) low frequency steady harmonics; (b) higher frequency range including time-varying harmonics

The spectrogram in Fig. 4 above shows some major vertical lines that correspond to transients of Type 2 and 3. The spectrogram is particularly useful in detecting such transients if a coarse enough frequency resolution is adopted, for a satisfactory accuracy in the time axis location. Transients may be identified and located by selecting a threshold on the non-characteristic components and, in particular, checking if more than one is above it. Two transients have been selected and further analyzed in Fig. 5, where the frequency resolution is 25 Hz, so to have a time window of 40 ms with a standard overlap of 50%; the overlap is necessary not only to better track time varying components, but also to artificially increase the time axis resolution. The last plot, in Fig. 6 was obtained with a 90% overlap, so that the time step is only 4 ms; it is possible to

distinguish the spectra before and after the transient event (dashed and dotted black curves), the spectra just at the beginning and the end of it (solid black curves) and during the transient itself (grey curves).

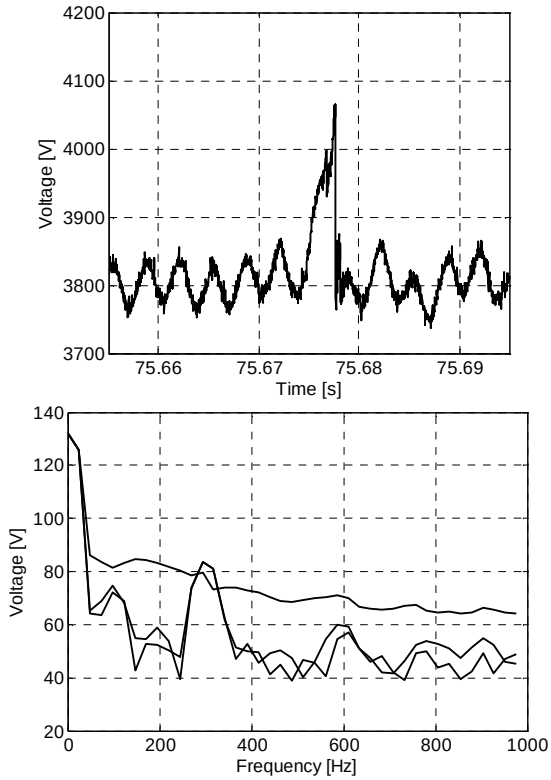

Figure 5. Spectrogram: transient waveform and Fourier spectra before, at and after the transient (20 ms time step)

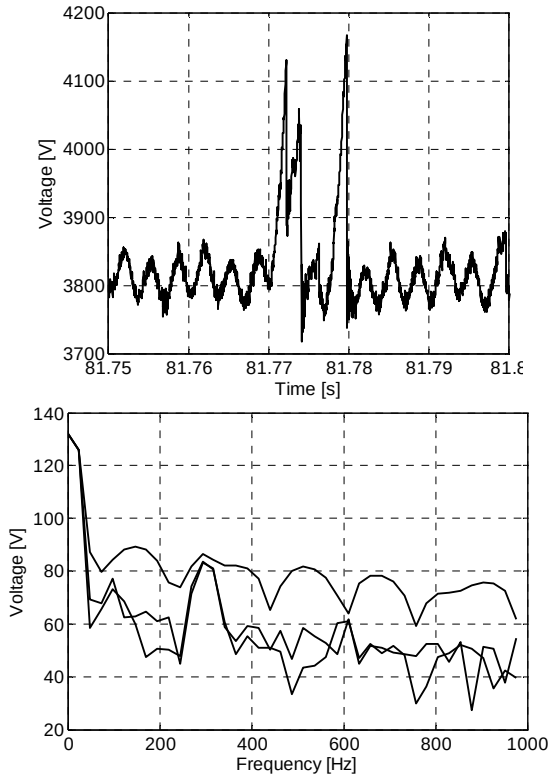

Figure 6. Spectrogram: transient waveform and Fourier spectra before, at and after the transient (20 ms time step)

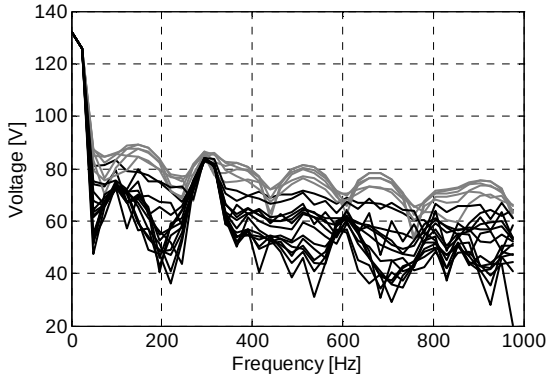

Figure 7. Spectrogram (refinement of the analysis of Fig. 6): spectra before (dashed black), partially including (solid black), centered at (solid gray) and after (dotted black) the transient (4 ms time step)

The use of overlapping (as well as zero padding of each time record) is able to improve the time axis resolution to a value the ensures transient detection; by observing the common transient durations (2 to 10 ms), a 50% overlap with 25 Hz resolution ensures a 20 ms time step and a uniform increase of frequency components by about 30%.

3.3. Wavelet analysis

The Discrete Time Wavelet Transform (DTWT) is at the moment preferred for its simplicity with respect to the Continuous Wavelet Transform, notwithstanding the better performances of the latter in terms of time and frequency resolution [16]. Transients in V_p are detected, by applying a threshold to the details d_k, and classified, by deriving empirical rules for the amplitude and number of oscillations in each detail channel. An example is shown in Fig. 8.

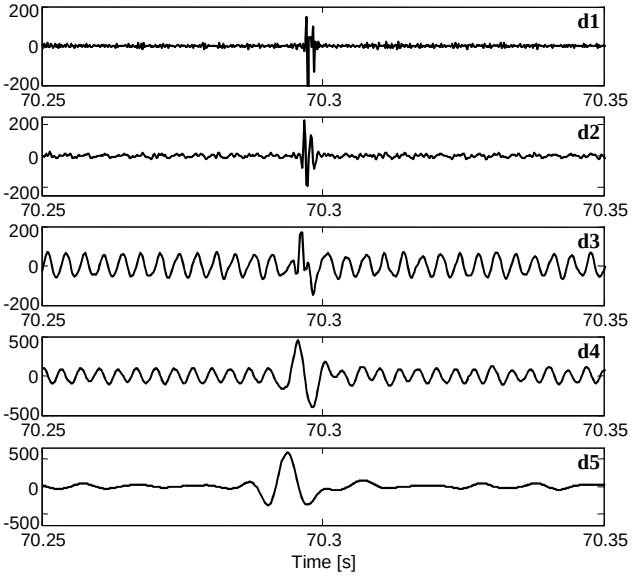

Figure 8. Example of V_p transient analyzed with *db3*, 5 levels wavelet

The details *d3* and *d4* show the 300 Hz ripple, that is removed from the adjacent ones. The detail d5 is considered as the best one from a signal-to-noise ratio point of view to identify a suitable threshold and locate transients due to pantograph bounces. It is remembered that pantograph bounces trigger the free response of the on-board filter and modify temporarily the behavior of the on-board chopper

and its conducted emissions, so that they represent a relevant event also for the evaluation of interference to signalling circuits and interoperability.

The Type 3 transient waveform located at 70.29 s as a result of the wavelet analysis (Fig. 8) is shown in Fig. 9: a pantograph bounce is superimposed to the steady V_p ripple due to substation harmonics (the main ripple visible in Fig. 5 is due to the 100 Hz component; the slight envelope modulation with ups and downs every two 100 Hz peaks is due to a residual 50 Hz component; the 300 Hz component is visible only as the repetitive jagging of the flanks of the 100 Hz ripple waveform).

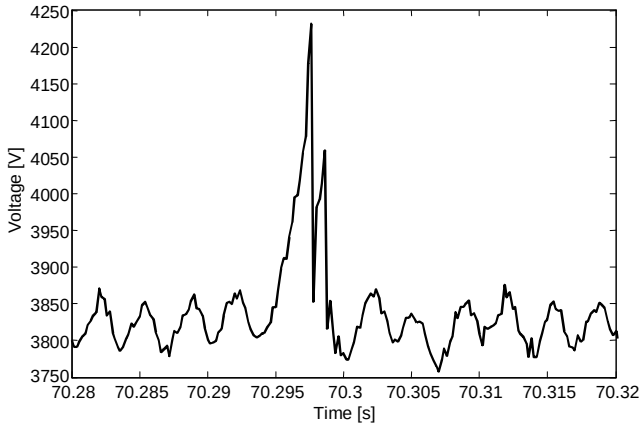

Figure 9. Waveform of the V_p transient analyzed in Fig. 8

The best mother wavelet is then selected by considering the largest amplitude of the peaks appearing in the details and the accuracy of their time location. Many mother wavelets produce almost identical results and only the main ones will be shown in the following discussion.

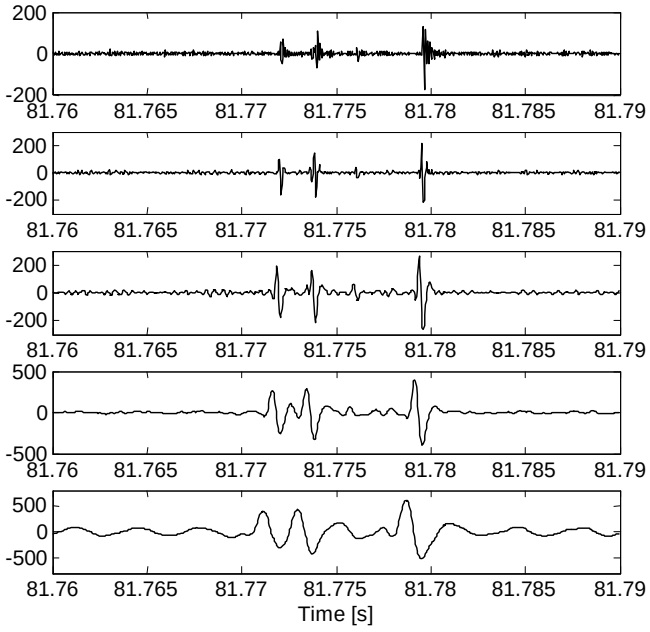

Figure 10. V_p transient of Fig. 6: *db3*, 5 levels wavelet

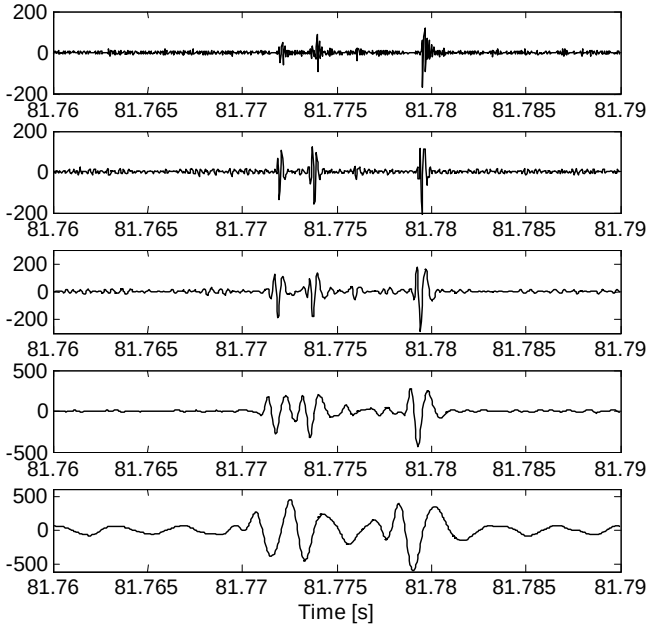

Figure 11. V_p transient of Fig. 6: *db5*, 5 levels wavelet

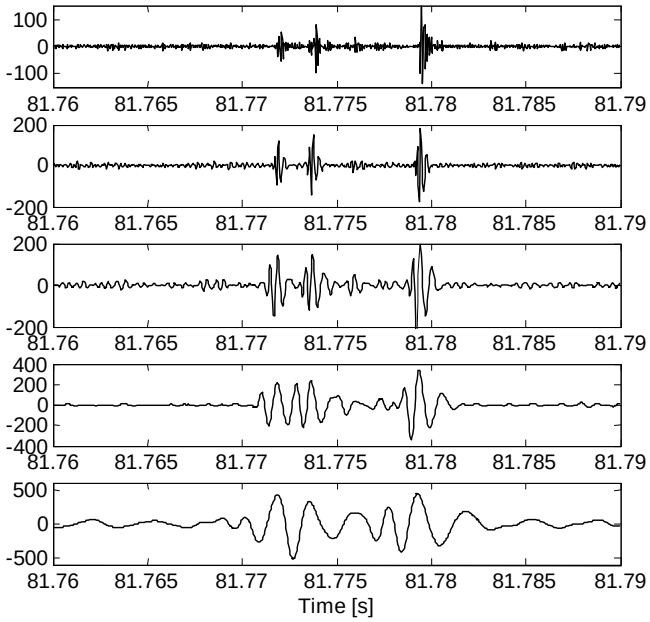

Figure 12. V_p transient of Fig. 6: *db8*, 5 levels wavelet (similar to *db10* and various high order *sym* wavelets)

Following [17] db4/db6 and db8/db10 were found the best choices for fast and slow transients, but for a different context, that of ac industrial supply networks. Low order wavelets may be not suited in general to follow all the variations of the analyzed signal, but they feature larger peak amplitude and allow an easier detection task. As an example, the results shown in Fig. 13 (obtained with a *db1* wavelet) show a 50% to 100% higher peaks in all details; moreover, the peaks are not oscillating, thus ensuring a better time axis location of the crossing of the applied threshold.

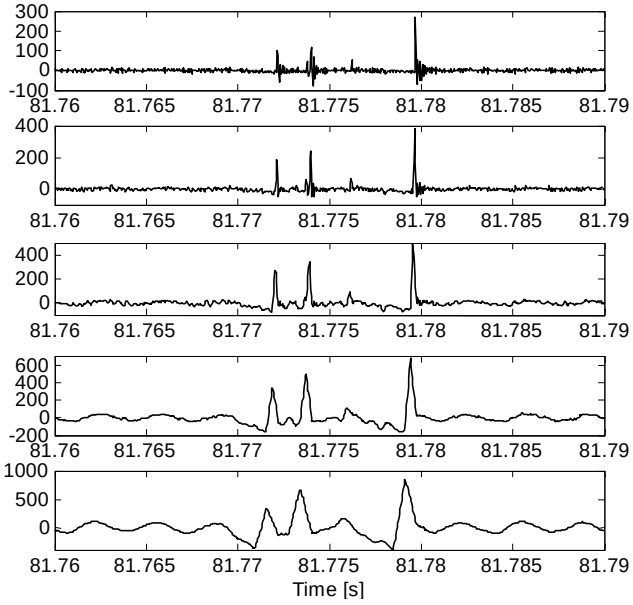

Figure 13. V_p transient of Fig. 6: *db1*, 5 levels wavelet (identical results for *sym1* and *haar* wavelets)

4. CONCLUSION

In the present paper a range of transients typical of dc railway systems are considered and classified for their time and frequency behavior. The target of the analysis is the evaluation of the power quality perceived at the pantograph voltage, but also the identification and location on the time axis of transients that are relevant also for interference to signalling circuits and thus for interoperability. The use of spectrogram and wavelets is proposed for the location of pantograph bounces on long records that cannot be inspected manually; the mother wavelets and types are selected and tested based on real signals. The results available in the literature that advise the optimal settings for wavelet analysis are almost always referred to ac distribution networks in industrial systems, while a dc railway system represent a peculiar case study. Very simple mother wavelet, such as those of order 1 and the Haar wavelet, seems preferable if accurate time axis location and fast computing are the main requisites.

REFERENCES

[1] A. Mariscotti, "Direct Measurement of Power Quality over Railway Networks with Results of a 16.7 Hz Network", *IEEE Trans. on Instrumentation and Measurement*, vol. 60 n. 5, May 2011, pp. 1604-1612.

[2] EN 50388, *Railway applications – Power supply and rolling stock – Technical criteria for the coordination between power supply (substation) and rolling stock to achieve interoperability*, Aug. 2005.

[3] EN 61000-4-7, *Electromagnetic compatibility – Part 4-7: Testing and measurement techniques – General guide on harmonics and interharmonics measurements and instrumentation, for power supply systems and equipment connected thereto*, 2002-08.

[4] EN 61000-4-17, *Electromagnetic compatibility – Part 4-17: Testing and measurement techniques – Ripple on d.c. input power port immunity test*, 1999-08.

[5] MIL STD 704E, "Aircraft electric power characteristics", May 1991.

[6] A. Mariscotti, "Analysis of the dc link current spectrum in voltage source inverters", *IEEE Trans. on Circuits and Systems - Part I*, vol. 49, n. 4, Apr. 2002, pp. 484-491.

[7] A. Mariscotti and P. Pozzobon, "Synthesis of line impedance expressions for railway traction systems", *IEEE Trans. on Vehicular Technology*, vol. 52 n. 2, March 2003, pp. 420-430.

[8] E.W. Kimbark, *Direct Current Transmission*, Wiley Interscience, 1971

[9] A. Mariscotti, "Methods for Ripple Index evaluation in DC Low Voltage Distribution Networks", IMTC 2007, Warsaw, Poland, May 2-4, 2007.

[10] S. Herraiz Jaramillo, G.T. Heydt and Efrain O'Neill-Carrillo, "Power Quality Indexes for Aperiodic Voltage and Currents", *IEEE Trans. on Power Delivery*, vol. 15, n. 2, pp. 784–790, April 2000.

[11] A. Mariscotti, Discussion of "Power Quality Indexes for Aperiodic Voltage and Currents", *IEEE Trans. on Power Delivery*, vol. 15, n. 4, Oct. 2000, pp. 1333-1334.

[12] FprEN 50238-2, "Railway applications – Compatibility between rolling stock and train detection systems – Part 2: Compatibility with Track Circuits", 2008-06.

[13] G. Armanino, A. Mariscotti and M. Mazzucchelli, "In-house test of low frequency conducted emissions of static converters for railway application", 17th IMEKO World Congress, Cavtat-Dubrovnik, Croatia, June 22-27, 2003.

[14] D. Bellan, A. Gaggelli, F. Maradei, A. Mariscotti and S. Pignari "Time-Domain Measurement and Spectral Analysis of Non-Stationary Low-Frequency Magnetic Field Emissions on Board of Rolling Stock", *IEEE Trans. on Electromagnetic Compatibility*, vol. 46 n. 1, Feb. 2004, pp. 12-23.

[15] A. Mariscotti, M. Ruscelli and M. Vanti, "Modeling of Audiofrequency Track Circuits for validation, tuning and conducted interference prediction", *IEEE Trans. on Intelligent Transportation Systems*, vol. 11 n. 1, March 2010, pp. 52-60.

[16] L. Angrisani, P. Daponte, M. D'Apuzzo, and A. Testa, "A measurement method based on the Wavelet Transform for power quality analysis", *IEEE Trans. on Power Delivery*, vol. 13 n. 4, Oct. 1998, pp. 990-998.

[17] S. Santoso, E.J. Powers, W.M. Grady and P. Hofman, "Power Quality assessment via Wavelet Transform analysis", *IEEE Trans. on Power Delivery*, vol. 11 n. 2, April 1996, pp. 924-930.